

## **An in situ Raman spectroscopic study of $\text{Na}_2\text{Si}_2\text{O}_5$ at high pressures and temperatures: Structures of compressed liquids and glasses**

**DANIEL L. FARBER\* AND QUENTIN WILLIAMS**

Department of Earth Sciences and Institute of Tectonics, University of California,  
Santa Cruz, California 95064, U.S.A.

### **ABSTRACT**

Raman spectra of  $\text{Na}_2\text{Si}_2\text{O}_5$  glass and  $\text{Na}_2\text{Si}_2\text{O}_5$  liquid have been collected in situ to pressures of 16 GPa at 300 K and 10 GPa at 885 K. In glass compressed at 300 K, bands associated with intertetrahedral bridging O atoms decrease in intensity and ultimately become unresolvable above 8 GPa. Over this same pressure range, new peaks appear in the glass between 600 and 800  $\text{cm}^{-1}$ ; these new features are consistent with the formation of  $\text{SiO}_3$  or  $\text{SiO}_6$  polyhedra through the destruction of nonbridging O atoms. Between  $\sim 10$  and 16 GPa, band intensities shift, the total integrated Raman scattering intensity of the glass decreases by more than a factor of ten, and the pressure dependence of mode shifts changes. These changes are consistent with a new densification mechanism initiated in the glass above  $\sim 8$  GPa, probably from the formation of linkages between two or more highly coordinated Si atoms. No vibrations attributed to bridged silica tetrahedra are observed in the liquid above 8 GPa, indicating that at least 50% of the Si in the liquid at 8 GPa is highly coordinated. Upon decompression of thermally quenched samples at 300 K, bands associated with bridged tetrahedra reappear at pressures below 1 GPa. Similarly, glasses that have been compressed only at 300 K and then decompressed have bands associated with bridged tetrahedra. The formation of bands associated with bridged tetrahedra on decompression both in glasses quenched from liquids formed at high-pressure and in glasses compressed at 300 K demonstrates that these species arise from structural reorganizations during decompression. Such reorganizations plausibly involve the breakdown of highly coordinated Si polyhedra and the resultant formation of bridged tetrahedra. The nearly complete decomposition of the high-pressure structure in glasses on decompression documents that in situ high-pressure measurements are crucial in deriving accurate constraints on the structure of silicate liquids at high pressure.

### **INTRODUCTION**

It is well known that many of the physical properties of magmas are controlled by their microstructure (Watson 1977; Ryerson and Hess 1978; Stolper et al. 1981; Mysen 1990). For example, densities, compressibilities, partitioning behavior, wetting characteristics, and viscosities of magmas are all dictated by the structural properties of silicate liquids. Thus, a detailed understanding of magmatic processes hinges critically on an understanding of the effects of pressure and temperature on liquid structure. There have been a reasonably large number of studies utilizing spectroscopic constraints to document the effect of changes in temperature on silicate liquid structure (Sweet and White 1969; Mysen and Frantz 1993, 1994; Brandriss and Stebbins 1988; Stebbins and Farnan 1989).

In contrast, evidence that pressure has a large effect on

the structure of silicate liquids has been derived largely through indirect techniques. Computer simulations (Angell et al. 1982; Matsui et al. 1982; Rustad et al. 1990, 1991) and analysis of fusion curves and phase equilibria (Burnham 1981; Irifune and Ohtani 1986; Knittle and Jeanloz 1989) indicate that profound structural changes occur in melts under compression. Measurements of density (Miller et al. 1991; Rigden et al. 1984, 1988; Agee and Walker 1993), viscosity (Kushiro 1976, 1980, 1986; Scarfe et al. 1987), and diffusivity (Shimizu and Kushiro 1984; Rubie et al. 1993; Watson 1979) of silicate melts document that each of these properties is a strong function of pressure. Yet, the precise structural changes that produce these pressure dependencies remain controversial.

Most experimental studies on the high-pressure structure of silicate liquids have been performed on glasses quenched from above the liquidus at high pressure and decompressed to ambient pressure. However, numerous studies have shown that high-pressure silicate and germanate glass structure is, in most cases, not quenchable

\* Present address: Department of Earth and Space Sciences, University of California, Los Angeles, California 90024, U.S.A.

to ambient pressure (Tischer and Drickamer 1962; Hemley et al. 1986b; Williams and Jeanloz 1988, 1989; Itie et al. 1989; Wolf et al. 1990; Durban and Wolf 1991; Meade et al. 1992; Williams et al. 1993; Cloosmann and Williams 1995). Ideally, such studies should be conducted by probing the liquid at simultaneous high pressure and temperature conditions. Yet, because of experimental difficulties, no such studies have been conducted on silicates. Previously, we documented coordination changes in a silicate-analog liquid ( $\text{Na}_2\text{Ge}_2\text{O}_5 \cdot \text{H}_2\text{O}$ ) at high pressure (Farber and Williams 1992); however, the relation of the high-pressure liquid structure to the glass formed from the liquid was unclear, since this composition crystallized when quenched.

Our present study is designed to examine the structural changes that take place in silicate melts at high pressures and temperatures and to characterize the structural differences between compressed liquids and pressurized and quenched glasses in a silicate system. In particular, we examine  $\text{Na}_2\text{Si}_2\text{O}_5$  liquids and glasses for three reasons. First, the composition  $\text{Na}_2\text{Si}_2\text{O}_5$  has a relatively low glass transition temperature (Kress et al. 1989; Mills 1972) and does not homogeneously nucleate crystals at ambient pressure (Zanotto and Weinberg 1989). Second, it is known to melt congruently up to pressures of 8 GPa (Kanzaki et al. 1989). Lastly, its density and viscosity have been studied on both glasses quenched from high pressure and on the liquid at high-pressure conditions (Scarfe et al. 1978). Thus, we expect that this composition should yield a homogeneous liquid at high pressure with neither refractory crystal contamination nor fractionation effects. In this study, we present data on amorphous  $\text{Na}_2\text{Si}_2\text{O}_5$  over a range of pressures and temperatures: These data represent the first in situ characterization of the structure of a silicate liquid at pressures corresponding to those in the deep upper mantle.

#### EXPERIMENTAL METHODS

The experiments were performed in Merrill-Bassett type diamond-anvil cells equipped with low fluorescence, type Ia diamonds with 750  $\mu\text{m}$  culets. All samples were contained in rhenium gaskets, and a small amount (<0.1% of the sample volume) of Sm:YAG was placed on the top diamond culet for pressure determination (Hess and Schiferl 1990); pressure variations across the  $\sim 250 \mu\text{m}$  diameter samples were less than  $\sim 1$  GPa at the highest pressure of this study ( $\sim 16$  GPa) and undetectable across distances comparable to the spot size ( $\sim 5 \mu\text{m}$ ) of the excitation laser. Following heating, our pressure gradients relaxed to <0.1 GPa. As with previous measurements on  $\text{Na}_2\text{Si}_4\text{O}_9$  glass (Wolf et al. 1990) no pressure medium was utilized; this lack of pressure medium is particularly important to avoid possible contamination of the sample at high temperatures. The Raman spectroscopic and external heating systems are described elsewhere (Kraft et al. 1991; Farber and Williams 1992). Our temperatures were measured using a thermocouple placed in contact with one of the anvils. This technique yields uncertainties

in temperature of  $\pm 5$  K (Farber and Williams 1992). The starting material was prepared from ultra-pure  $\text{SiO}_2$  and  $\text{Na}_2\text{CO}_3$  (Johnson and Matthey), which were ground under ethanol and then melted in a platinum crucible for 30 min at 1573 K, followed by rapid quenching in air. The resulting glass was then reground and refused three times to ensure homogeneity; it was stored at 388 K until loading into the cell. Glass fragments were optically clear, indicating that no significant hydration of the sample had occurred. However, the presence of a weak shoulder at  $\sim 900 \text{ cm}^{-1}$  in our ambient pressure spectrum suggests that minor surface hydration could have occurred. This feature was not present in our high-pressure spectra. To characterize the homogeneity of these glasses, Raman spectra were collected from multiple  $\sim 1$  mm chips. The intensity ratio of the Raman bands at 1100 and  $950 \text{ cm}^{-1}$  has been shown to be a strong function of composition (Furukawa et al. 1981). The relative amplitudes and full widths at half maximum of these bands were fitted using a nonlinear optimization algorithm, which was utilized in the analysis of all our spectra (Farber and Williams 1992). This yielded both peak amplitudes and half-widths for our starting material that were indistinguishable from previous work on  $\text{Na}_2\text{Si}_2\text{O}_5$  glass (Brawer and White 1975; Furukawa et al. 1981). From the trends of peak amplitude ratios and half-widths with composition determined by Brawer and White (1975), the Na/Si ratio in our glasses can be constrained to be within 5% of the disilicate composition.

Liquid spectra were collected by compressing  $\text{Na}_2\text{Si}_2\text{O}_5$  glass and then heating to a final experimental temperature. The sample temperature was increased at  $\sim 10$  K/min in 100 K intervals, with the sample being held at each interval for a minimum of 30 min. Upon completion of the high-temperature portion of the experiment, the cell was quenched in air to below the glass transition in <1 min. Because of thermal relaxation of the cell assembly, the final experimental pressure was as low as 80% of the initial sample pressure.

Because experiments at temperatures above  $\sim 885$  K resulted in heterogeneous nucleation and rapid growth of crystals in our samples, the final experimental temperatures were carefully chosen to be as high as possible without inducing crystallization over the timescales of our experiments. In all the high-temperature liquid spectra that we present, none of the characteristic sharp Raman peaks of sodium silicate crystals was observed, nor were any crystals observed optically.

The temperature at which glasses relax structurally is a strong function of the time at which they are held at a temperature (cf. Brawer 1985). Our samples (which were held at their maximum experimental temperatures for  $> 10^3$  s) would relax to a supercooled liquid at ambient pressure at  $\sim 700$  K (Kress et al. 1989; Mills 1972). For comparison, our maximum temperature is 885 K at pressures of 10 GPa. Accordingly, unless the structural relaxation temperature of the compressed glass has a strong positive pressure dependence, our results were clearly

conducted within a relaxed regime. In  $\text{Na}_2\text{Si}_2\text{O}_5$  liquid, viscosity decreases at pressures greater than 1.5 GPa, whereas in alkali silicates ranging in composition from  $\text{Na}_2\text{Si}_2\text{O}_5$  to  $\text{Na}_2\text{Si}_4\text{O}_9$ , viscosity has been demonstrated to decrease at pressures up to 10 GPa (Scarfe et al. 1978, 1987; Kushiro 1976, 1986; Rubie et al. 1993). This general decrease at high pressures suggests that the structural relaxation temperature may actually decrease over this pressure range (Angell and Sichina 1976; Gupta 1987). This conclusion is also in accord with the positive correlation observed between  $T_g$  and viscosity in sodium silicate melts at high pressure (Rosenhauer et al. 1978). Further evidence that our high-temperature spectra were collected in a relaxed regime is shown by spectra collected at 10 GPa and 775 and 885 K (Fig. 1). These spectra are strikingly similar but differ significantly from spectra collected at 300 K, which further indicates that by 775 K the structure has fully relaxed.

### RESULTS

The structure of alkali-silicate glasses formed at ambient pressure has been extensively studied. At low pressure, the structure of such glasses can be described in terms of a three-dimensional tetrahedral network, modified by the presence of alkali cations. Although the short-range structure (first nearest-neighbor) may be quite regular, the exact nature of the tetrahedral linkages is strongly dependent on the alkali content of the glass. The structure of the tetrahedral network is commonly described in terms of the number of bridging O atoms per tetrahedron ( $n$ ), or  $Q^n$  species. With the addition of alkalis, the structure becomes increasingly depolymerized and becomes a mixture of a range of Q species. For disilicates, the glass has an average of three bridging and one nonbridging O atom per tetrahedron ( $Q^3$ ).

Because our interpretation depends crucially upon the assignment of peaks in the spectrum of alkali-silicate glasses, we briefly review the important features of these spectra, along with plausible spectral assignments. We utilize primarily the assignments derived by Brawer and White (1975) and Furukawa et al. (1981) from studies of a range of glasses in the  $\text{Na}_2\text{O-SiO}_2$  system, coupled with simple force-constant calculations. The Raman spectroscopic features of alkali-silicate glasses are most easily understood in terms of increasing deviation from the spectrum of vitreous silica with increasing alkali content. As alkali content is increased: (1) The dominant broad band centered at  $435\text{ cm}^{-1}$  in vitreous silica decreases in intensity until the  $\text{Na}_2\text{Si}_3\text{O}_7$  composition is reached, where it becomes a weak shoulder; (2) a narrow band near  $520\text{ cm}^{-1}$  appears and shifts to higher frequency; (3) a weak band near  $800\text{ cm}^{-1}$  decreases in both frequency and intensity and becomes more symmetric; (4) a band appears at  $1070\text{ cm}^{-1}$  and shifts to higher frequency, reaching a maximum in intensity at the disilicate composition; and (5) a band appears at  $980\text{ cm}^{-1}$  and progressively shifts to lower energy (Brawer and White 1975; Furukawa et al. 1981; Matson et al. 1983). The strong band near  $1100$

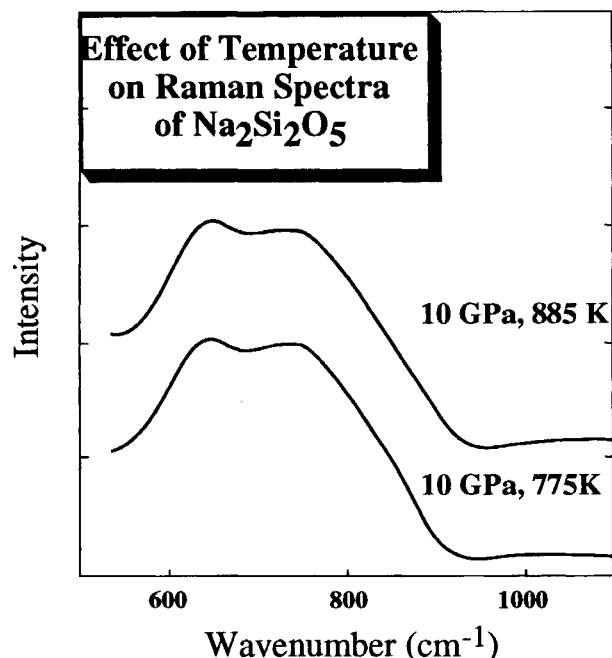


FIGURE 1. Effect of temperature on the Raman spectra of liquid  $\text{Na}_2\text{Si}_2\text{O}_5$  at 10 GPa.

$\text{cm}^{-1}$  is attributed to the symmetric stretching of  $Q^3$  species, in accord with its high intensity in the disilicate composition, whereas the weak band at  $\sim 980\text{ cm}^{-1}$  in  $\text{SiO}_2$  is attributed to the symmetric stretching of  $Q^2$  species. The weak band at  $\sim 800\text{ cm}^{-1}$  in  $\text{SiO}_2$  has been interpreted as resulting from Si motion within the O framework (Galeener and Mikkelsen 1981; Galeener and Geissberger 1983); this band shifts to near  $770\text{ cm}^{-1}$  in the disilicate composition. The slightly lower (between  $400$  and  $700\text{ cm}^{-1}$ ) frequency region of the spectrum of alkali-silicate glasses at ambient pressure arises largely from bending-type motions of the Si framework. The dominant band at  $570\text{ cm}^{-1}$  in  $\text{Na}_2\text{Si}_2\text{O}_5$  glass is most likely produced by Si-O-Si bending motions of  $Q^3$  species, whereas the weak shoulder on the low frequency side of this band has been attributed to bending vibrations of  $Q^4$  species (Fig. 2). The shoulder present at  $\sim 630\text{ cm}^{-1}$  has been attributed either to Si-O-Si bending motions from species with tight Si-O-Si angles or to a combined bending and stretching vibration of  $Q^2$  species (Furukawa et al. 1981; McMillan 1984), as well as to vibrations of three-membered rings (note, however, that these assignments are not exclusive: Matson et al. 1983; Dickinson et al. 1990; Sharma et al. 1981; Galeener 1982; Galeener and Geissberger 1983; Revesz and Walrafen 1983; Barrio et al. 1993; Kubicki and Sykes 1993). Yet, the lack of sharpness of this feature suggests that a distribution of Si-O-Si angles gives rise to this shoulder; thus, if it is generated by three-membered rings, it is likely that they are somewhat variable in their distortion.

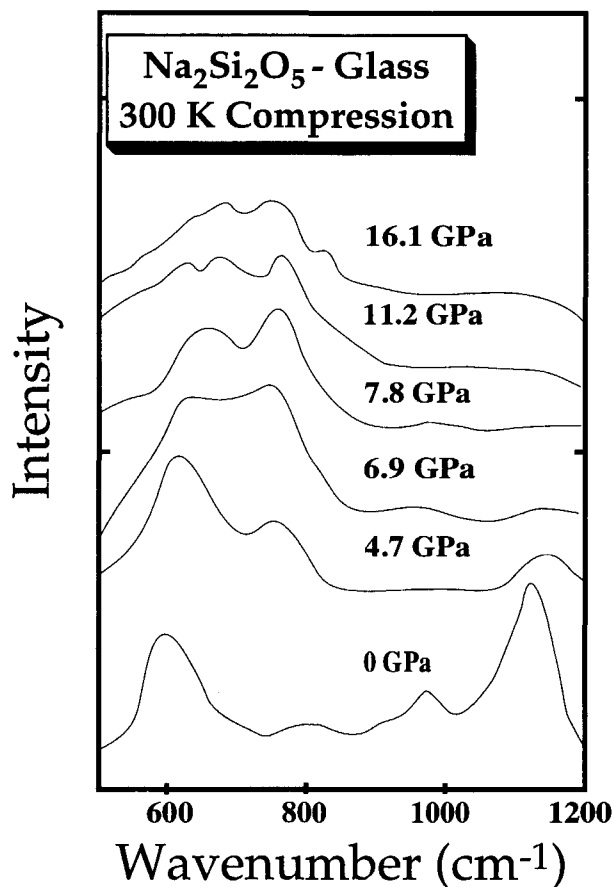


FIGURE 2. Representative Raman spectra of  $\text{Na}_2\text{Si}_2\text{O}_5$  glass under compression. The pressures indicate the actual conditions under which the data were collected. All the spectra have been normalized such that the height of the feature appearing between 570 and  $\sim 700\text{ cm}^{-1}$  is approximately constant among spectra. Relative to the low-pressure spectra, the intensities of the spectra at the two highest pressures are multiplied by about a factor of ten.

#### COMPRESSION OF $\text{Na}_2\text{Si}_2\text{O}_5$ GLASS AT 300 K

Figure 2 shows Raman spectra of  $\text{Na}_2\text{Si}_2\text{O}_5$  glass under compression at 300 K. Between 0 and 8 GPa the most marked trend in these spectra is the rapid decrease in the absolute intensity of both the  $\sim 1100$  and  $\sim 950\text{ cm}^{-1}$  bands until they ultimately become unresolvable. Over this same pressure range a band centered at  $\sim 750\text{ cm}^{-1}$  grows in intensity with compression. Between 5 and 8 GPa, this band becomes the dominant feature in the spectrum, gaining intensity relative to a band near  $\sim 600\text{ cm}^{-1}$ . Above 8 GPa, there is a distinct change in the character of the spectra, with the band near  $\sim 600\text{ cm}^{-1}$  broadening and increasing in intensity. The mode shifts of the peaks also change near 8 GPa (Fig. 3). Finally, the overall Raman scattering intensity decreases by approximately an order of magnitude between  $\sim 8$  and  $\sim 12$  GPa. At pressures in excess of 10 GPa there is evidence that separate

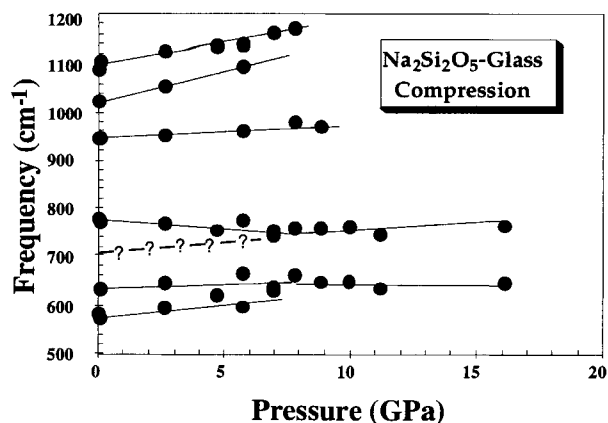


FIGURE 3. Pressure dependence of the Raman bands of  $\text{Na}_2\text{Si}_2\text{O}_5$  glass. All data were collected under compression. Errors in the peak positions from our deconvolution are estimated to be  $<10\text{ cm}^{-1}$  for the low-pressure data ( $<8\text{ GPa}$ ) and  $<20\text{ cm}^{-1}$  for the data above  $\sim 8\text{ GPa}$ . The solid lines are drawn as a guide for the eye.

structural environments evolve in the glass; the mode at  $600\text{ cm}^{-1}$  appears to split into two components and a shoulder evolves on the high energy side of the  $800\text{ cm}^{-1}$  peak.

At ambient pressure, the high-frequency ( $>800\text{ cm}^{-1}$ ) Raman spectrum of  $\text{Na}_2\text{Si}_2\text{O}_5$  glass is easily understood in terms of vibrational modes involving stretching vibrations of Si in tetrahedral coordination. The decline in intensity in this spectral region implies that at high pressures densification mechanisms involving coordination changes of Si are likely to be important. We cannot absolutely preclude that large and unexpected pressure-induced changes in the Raman scattering cross-section of silica tetrahedra could give rise to this decrease in intensity. However, pressure-induced changes in Raman band intensities have been noted in glasses primarily when major structural changes occur (such as coordination changes) (e.g., Hemley et al. 1986b; Durban and Wolf 1991; Williams et al. 1993). Nor is such a decrease in Raman scattering intensity observed under compression in crystalline phases containing silica tetrahedra (e.g., Hemley 1987).

Among crystalline phases, stishovite,  $\text{MgSiO}_3$ -ilmeneite, and  $\text{MgSiO}_3$ -perovskite all have strong vibrational bands between 750 and  $800\text{ cm}^{-1}$ , a region associated with stretching motions of the  $\text{SiO}_6$  group (Hemley et al. 1986a; McMillan and Ross 1987; Williams et al. 1987). Bending motions of  $\text{SiO}_6$  groups produce Raman bands between 540 and  $590\text{ cm}^{-1}$  at ambient pressure in  $\text{MgSiO}_3$ -perovskite and stishovite (Hemley et al. 1986a; Williams et al. 1987). We therefore attribute the loss of intensity of the  $\sim 1100$  and  $\sim 950\text{ cm}^{-1}$  bands between 0 and 8 GPa to the breakdown of the regular tetrahedral network of the glass, coupled with the production of initially small amounts of highly coordinate Si within the

glass. Concomitant with the loss of intensity in these Q<sup>3</sup> and Q<sup>2</sup> vibrations, bands at both ~750 cm<sup>-1</sup> and the region near 600 cm<sup>-1</sup> dramatically increase in amplitude. Although the mode shifts (Fig. 3) suggest that the band initially at ~770 cm<sup>-1</sup> decreases in frequency with pressure, we interpret this shift as being produced by a superposition of two bands of differing pressure shifts. The apparent decrease in frequency of this band appears to arise from the pressure-induced growth of a broad band at lower frequency than the band that appears near ~770 cm<sup>-1</sup> at low pressures. The relatively weak low-pressure feature at ~770 cm<sup>-1</sup> is probably produced by bending of the Si-O-Si bond angle, which is induced primarily by displacement of the bridging O atom between silica tetrahedra and only minimally by Si motion (e.g., McMillan et al. 1994). At higher pressures we attribute the strong band in this region (and its associated high frequency shoulder in our highest pressure spectrum of Fig. 2) to the symmetric stretching vibration of SiO<sub>6</sub> octahedra. This assignment is consistent with the assignment of new Raman bands produced on compression of GeO<sub>2</sub> and Na<sub>2</sub>Si<sub>4</sub>O<sub>9</sub> glasses (Wolf et al. 1990; Durban and Wolf 1991) and also with the known spectra of SiO<sub>6</sub>-bearing crystalline phases.

The shoulder in Na<sub>2</sub>Si<sub>2</sub>O<sub>5</sub> glass near 630 cm<sup>-1</sup> in the ambient pressure spectrum has a low-pressure mode shift, which suggests that this feature should lie near 670 cm<sup>-1</sup> at 8 GPa (Fig. 3). Thus, the intense feature that is present near 630 cm<sup>-1</sup> at pressures of 8 GPa and above may not have the same origin as the feature present at this location in the low-pressure spectra. The initial increase in intensity near ~600 cm<sup>-1</sup> between 0 and 8 GPa and the loss of intensity of the Q<sup>2</sup> and Q<sup>3</sup> bands could be caused by the production of narrowed Si-O-Si angles or three-membered rings through the formation of SiO<sub>5</sub> or SiO<sub>6</sub> polyhedra connected with Q<sup>4</sup> tetrahedra (Wolf et al. 1990). Although we cannot absolutely preclude that three-membered rings of tetrahedra give rise to the ~630 cm<sup>-1</sup> band in our spectra above 8 GPa, we note that such three-membered rings would be required to have unresolvably weak tetrahedral stretching vibrations in the 900–1100 cm<sup>-1</sup> region. As bands in this region are a primary vibrational characteristic of essentially all known silicate tetrahedra-bearing species containing nonbridging O atoms, we attribute this band instead to bending motions of more highly coordinated silica species. This latter assignment is therefore entirely consistent with the observation that the intensity of the ~630 cm<sup>-1</sup> band is anticorrelated with the intensity of the bands produced by known tetrahedral species in the 900–1100 cm<sup>-1</sup> region. Therefore, the enhancement in the intensity of this band is plausibly produced by an increased concentration of highly coordinated species as pressure is increased. We note also that the assignment of this band to highly coordinated Si is identical to that utilized by Wolf et al. (1990) to explain a similar pressure-induced enhancement of a band at this location in Na<sub>2</sub>Si<sub>4</sub>O<sub>9</sub> glass between 0 and 18 GPa.

There are two crucial aspects of our assignments of the 630 and 750 cm<sup>-1</sup> features in our spectra above 8 GPa to highly coordinated Si. First, the mode shifts of these features are discontinuous with those of the bands present near (but offset from) these locations in the ambient pressure glass (features that we would expect to lie at markedly different frequencies at high pressures). Second, the broadening of these features, as well as the fact that they are the most intense features in our spectra, correlates precisely with the dramatic decline in intensity of the tetrahedral stretching bands associated with Q species within the glass. Such an apparent lack of bands produced by Q species is completely unknown for a glass of this chemistry, and the most plausible explanation for our spectral observations is simply that the tetrahedra in the glass are no longer present at high-pressure conditions.

The reason that such profound structural reorganizations occur at lower pressures in Na<sub>2</sub>Si<sub>2</sub>O<sub>5</sub> glass rather than Na<sub>2</sub>Si<sub>4</sub>O<sub>9</sub> glass can be understood in terms of the role of nonbridging O atoms. The formation of dense Na<sub>2</sub><sup>16</sup>Si<sub>2</sub>O<sub>5</sub> or Na<sub>2</sub><sup>16</sup>SiO<sub>3</sub> structures at low temperatures appears to be accomplished most efficiently through the conversion of a nonbridging O atom to a bridging O atom between a highly coordinated Si and a tetrahedral Si (Wolf et al. 1990). That is, an initially nonbridging O atom enters the coordination sphere of a neighboring Si atom. The formation of highly coordinated Si through such reactions was also observed in recent molecular dynamic simulations of silicate liquids at high pressures (Kubicki and Lasaga 1991). The fact that these coordination-changing reactions appear to take place at lower pressure in Na<sub>2</sub>Si<sub>2</sub>O<sub>5</sub> glass may simply be a consequence of the greater abundance of nonbridging O atoms in glasses of this composition.

Between 8 and 16 GPa a new densification mechanism is initiated in Na<sub>2</sub>Si<sub>2</sub>O<sub>5</sub> glass. This mechanism probably involves the formation of <sup>16</sup>Si-<sup>13</sup>O-<sup>16</sup>Si linkages or <sup>15</sup>Si-<sup>13</sup>O-<sup>16</sup>Si linkages. The loss of intensity in the bands associated with SiO<sub>4</sub> units and the broadening and overall loss of the Raman-scattered intensity in the 700 cm<sup>-1</sup> region are similar to effects seen in Na<sub>2</sub>Si<sub>4</sub>O<sub>9</sub>, SiO<sub>2</sub>, and GeO<sub>2</sub> glasses at high pressures (Wolf et al. 1990; Hemley et al. 1986b; Williams et al. 1993; Durban and Wolf 1991). Such changes have been uniformly associated with the formation of octahedrally coordinated Si or Ge. Indeed, the correlation of peak broadening and loss of integrated Raman scattering intensity with the initiation of coordination changes in both SiO<sub>2</sub> (Hemley et al. 1986b; Williams et al. 1993) and GeO<sub>2</sub> (Durban and Wolf 1991) glasses, as measured with X-ray scattering (Meade et al. 1992) and EXAFS (Itie et al. 1989), has been demonstrated robustly in these two network glasses. In addition, the onset of significant broadening of the Raman spectra of Na<sub>2</sub>Si<sub>4</sub>O<sub>9</sub> glass occurs at the same pressure at which bands associated with Q<sup>2</sup> and Q<sup>3</sup> species are lost (Wolf et al. 1990). The simultaneous loss of the bands associated with Q species and the initiation of significant band broadening in Na<sub>2</sub>Si<sub>2</sub>O<sub>5</sub> above ~10 GPa suggest that the local

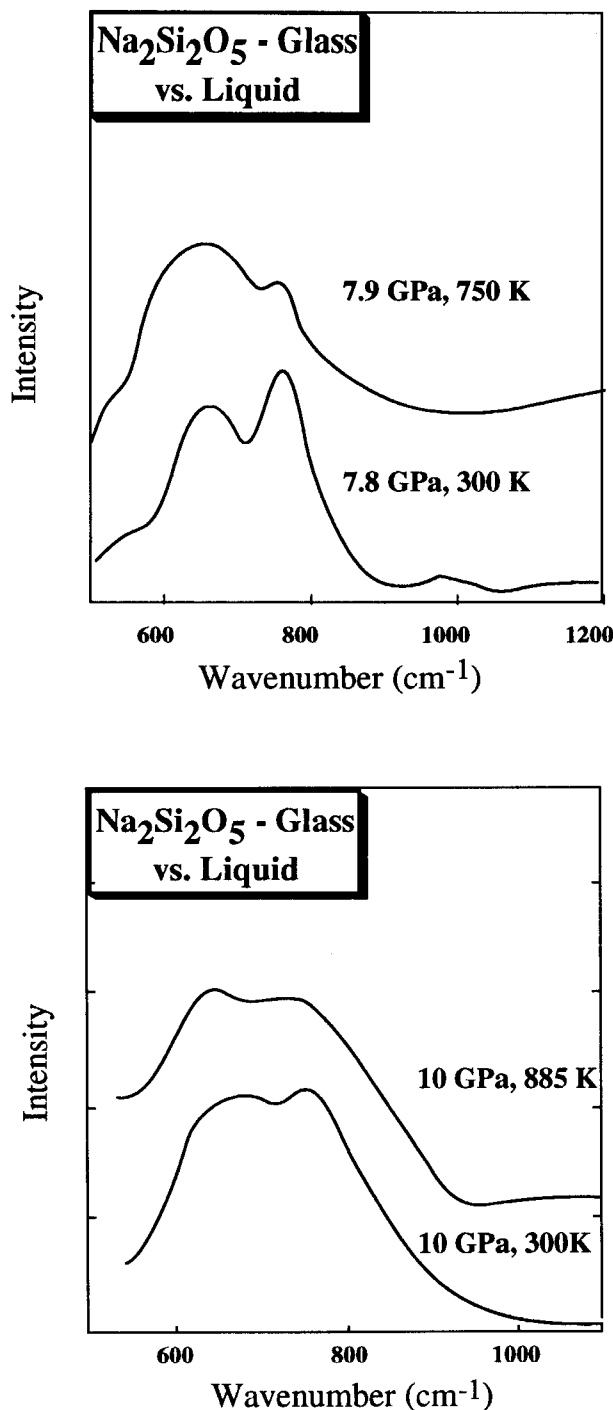


**FIGURE 4.** Representative in situ Raman spectra of liquid  $\text{Na}_2\text{Si}_2\text{O}_5$  collected at 7.9 GPa and 750 K and at 10.3 GPa and 885 K, and  $\text{Na}_2\text{Si}_2\text{O}_5$  glass compressed at 300 K to 7.8 GPa and 10.3 GPa. Note the marked change in relative intensity between the bands centered at  $\sim 650$  and  $\sim 750$   $\text{cm}^{-1}$ .

environment around Si is similar to that found in  $\text{Na}_2\text{Si}_4\text{O}_9$  (and  $\text{SiO}_2$ ) glasses at somewhat higher pressures. It is likely that these similar spectral responses are associated at least with the complete conversion of nonbridging O atoms to highly coordinated species in these compositions and profound alteration of the low-pressure tetrahedral network. In  $\text{Na}_2\text{Si}_2\text{O}_5$ , such complete conversion of nonbridging O atoms to O atoms that bridge between a  $^{69}\text{Si}$  and a  $^{49}\text{Si}$  results in a minimum presence of 50% of the Si (which could be expressed in terms of components as  $\text{Na}_2^{69}\text{SiO}_3 + ^{49}\text{SiO}_2$ ) in highly coordinated polyhedra. Thus, we are able to obtain a bound on the structure of the glass if the disappearance of Raman peaks associated with formal Q species is associated with the annihilation of O atoms bridged between two  $^{49}\text{Si}$  atoms.

#### STRUCTURE OF $\text{Na}_2\text{Si}_2\text{O}_5$ GLASS AND LIQUID AT HIGH PRESSURE

In Figure 4, we compare spectra collected at 8 and 10 GPa for liquid  $\text{Na}_2\text{Si}_2\text{O}_5$ , to that of the isochemical glass compressed to the same pressure at 300 K. Major differences exist between the glass spectrum collected at 300 K and the liquid spectra collected at high temperature. Within the liquid the strong band at  $\sim 750$   $\text{cm}^{-1}$  is lower in amplitude, and the band at  $\sim 650$   $\text{cm}^{-1}$  is more intense and shifted to lower energy. Although we are able to resolve a weak band associated with  $\text{Q}^3$ -linked tetrahedra at 1170  $\text{cm}^{-1}$  (Fig. 3; note that this feature shifted under pressure from near 1100  $\text{cm}^{-1}$  at ambient conditions) in the spectra of the glass at 7.8 GPa, no feature is resolvable at this location in the liquid spectra collected at the same pressure. Therefore, the disappearance of formal Q species may occur at somewhat lower pressures in the liquid than in the glass.

Figure 4 shows that the population of dense structures present at high temperature at 8 and 10 GPa exceeds that present in the glass at comparable pressures (as manifested by the change in amplitude of the peak at 600  $\text{cm}^{-1}$ ). Indeed, the structure of the liquid at 8 GPa is more similar to that of the glass compressed to 11 GPa at 300 K (Fig. 2) than to the glass compressed to 8 GPa. In the 300 K glass at 11 GPa, the feature at  $\sim 750$   $\text{cm}^{-1}$  is only a shoulder on the  $\sim 600$   $\text{cm}^{-1}$  band, whereas in the liquid these bands are both still distinct, with the  $\sim 600$   $\text{cm}^{-1}$  band considerably more intense. This narrower peak width in the liquid suggests that the highly coordinated Si polyhedra in  $\text{Na}_2\text{Si}_2\text{O}_5$  liquid are more structurally uniform and less distorted than those within the isochemical glass. A drastic change in intensity of Raman bands in liquids while maintaining uniform peak widths (and thus presumably structurally discrete environments) was also observed in alkali-germanate melts under pressure (Farber and Williams 1992). Thus, the presence of locally well-defined and structurally discrete first-neighbor environments may be a general feature of silicate liquids undergoing coordination changes.

### EFFECTS OF DECOMPRESSION ON GLASSES FORMED AT HIGH PRESSURE

Spectra of glasses quenched to ambient conditions after heating at high pressure and after simple compression at 300 K are shown in Figure 5. The spectrum of the glass formed following compression to 11 GPa and quenched to ambient pressure shows that the bands associated with  $^{16}\text{Si}$  regain virtually all their original intensity on decompression. In the glass spectra collected at high pressure (Fig. 2) no bands were present at either  $\sim 950$  or  $\sim 1100$   $\text{cm}^{-1}$  ( $\text{Q}^2$  and  $\text{Q}^3$  species) at the highest pressures experienced by this glass; in the pressure-quenched glass, these features dominate the spectrum. Similar behavior was observed in  $\text{Na}_2\text{Si}_4\text{O}_9$  glass quenched from high pressure in which most of the intensity of these tetrahedral features returned at pressures below 1 GPa (Wolf et al. 1990). Such reversion of highly coordinated structures on decompression has been observed in a wide range of silicate and silicate-analog glasses (Hemley et al. 1986b; Williams and Jeanloz 1988; 1989; Itie et al. 1989; Wolf et al. 1990; Durban and Wolf 1991; Williams et al. 1993).

There are small but significant differences between the glass compressed to high pressures and the glass formed at ambient pressure. The amplitude of the  $\sim 1100$   $\text{cm}^{-1}$  band decreases slightly relative to the  $\sim 950$   $\text{cm}^{-1}$  band, and the  $\sim 600$   $\text{cm}^{-1}$  shoulder increases slightly in intensity. For comparison, in  $\text{Na}_2\text{Si}_4\text{O}_9$  glass Wolf et al. (1990) found that a strong band at  $598$   $\text{cm}^{-1}$  appeared on quenching in a glass compressed to 13 GPa, whereas we observe only a minor increase in the intensity of the shoulder at  $600$   $\text{cm}^{-1}$ . If this feature is associated with three-membered rings of tetrahedra, then the smaller degree of polymerization of our glasses plausibly explains the lowered amplitude of this band. However, the differences we observe between glasses quenched from elevated pressure and ambient pressure glasses are clearly not a direct consequence of the response of the structure to compression; rather, they represent the response of the high-pressure glass structure to decompression-induced expansion. Thus, constraints on high-pressure glass structure derived only from the study of quenched glasses are likely to be fraught with uncertainties because of major structural changes occurring on decompression.

In fact, we can evaluate how accurately the structure of quenched  $\text{Na}_2\text{Si}_2\text{O}_5$  glasses formed from liquids at high pressure represents the high-pressure liquid structure. The spectrum of the glass produced by quenching the liquid equilibrated at 8 GPa and 750 K to ambient conditions is consistent with a largely tetrahedrally coordinated glass, in contrast to its spectrum at high pressures and temperatures (Figs. 4 and 5). Again, this spectrum shows a close resemblance to that of the glass formed at ambient pressure. Yet, as in the glass that had been compressed only, the peak at  $\sim 950$   $\text{cm}^{-1}$  associated with  $\text{Q}^2$  species is higher in amplitude than in the untreated glass, suggesting that the relative proportion of  $\text{Q}^2$  species is higher in both

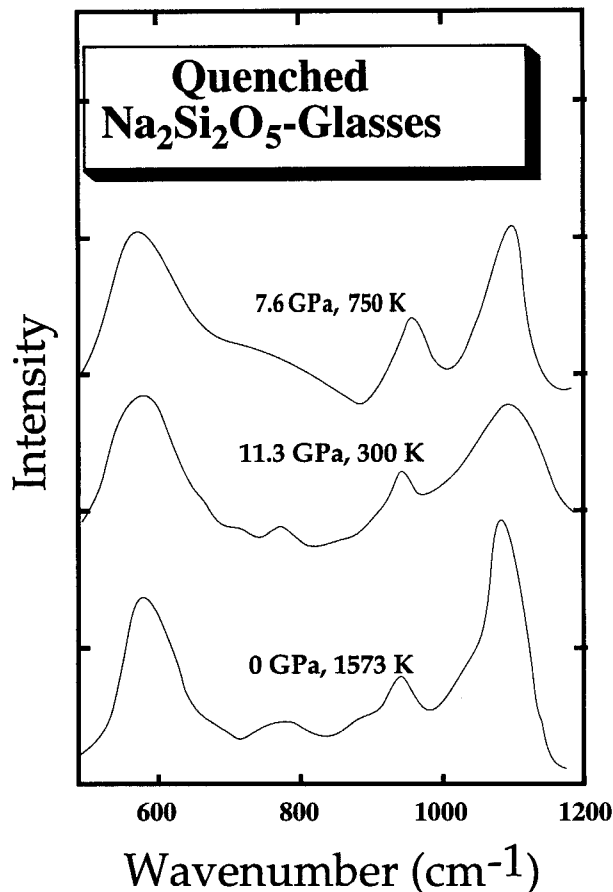


FIGURE 5. Raman spectra of quenched  $\text{Na}_2\text{Si}_2\text{O}_5$  glasses collected at ambient pressure. Labels give the conditions from which the glasses were quenched. Note the increase in amplitude of the band at  $\sim 950$   $\text{cm}^{-1}$  relative to that at  $\sim 1100$   $\text{cm}^{-1}$  in the glasses quenched from high pressure.

the heated and unheated glasses quenched from high pressures. There is also more intensity in a broad feature centered at  $\sim 780$   $\text{cm}^{-1}$ , probably associated with Si-O-Si bending motions (Galeener and Geissberger 1983; McMillan 1984). This vibration tends to increase in intensity with decreasing Si-O-Si bond angles (Furukawa et al. 1981), and we accordingly expect its intensity to be augmented in the pressurized glasses (Hemley et al. 1986b; Williams and Jeanloz 1988; Xue et al. 1993). The presence of  $\sim 2\%$  highly coordinated Si in  $\text{Na}_2\text{Si}_2\text{O}_5$  glass quenched from conditions near 8 GPa and 750 K (Xue et al. 1991) suggests that some intensity in this spectral range could be produced by the vibration of an O atom bridging  $^{16}\text{Si}$  and  $^{14}\text{Si}$ . Thus, in the glass formed from a compressed liquid the increase in the intensity of this band reflects the presence of either dense tetrahedral linkages produced during decompression, as manifested by narrowed Si-O-Si bond angles, or the preservation of minor amounts of  $^{16}\text{Si}$ .

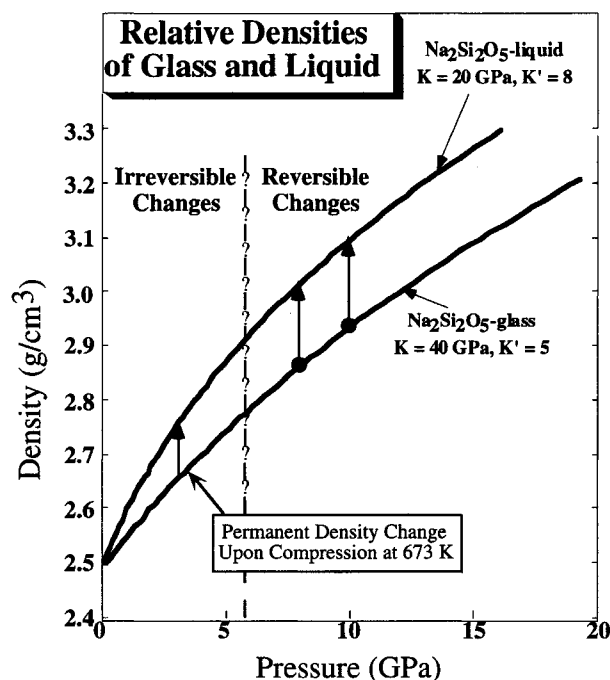


FIGURE 6. Density vs. pressure relations for compression of  $\text{Na}_2\text{Si}_2\text{O}_5$  liquid and glass, using bulk moduli from White et al. (1977) and Kress et al. (1988). We assume that  $K'$ , the pressure derivative of the bulk modulus, is  $\sim 8$  for the liquid and 5 for the glass. Our assumed values of  $K'$  do not notably influence the relative equations of state until  $\sim 7$  GPa. The queried line marks the approximate boundary between the reversible densification mechanisms documented in this study and the irreversible changes that lead to the permanent densification seen in studies at lower pressures and temperatures (Uhlmann 1973/1974).

## DISCUSSION

We have demonstrated that the structure of liquids at high pressure bears little resemblance to the spectra of glasses quenched to ambient conditions. We do not preclude that minor amounts of dense features may exist in quenched glasses (e.g., 2–5% <sup>16</sup>Si in alkali silicate glasses quenched from 5 to 9 GPa; Xue et al. 1991). Rather, we simply observe that most structural features of quenched glasses are entirely different from the structures observed at actual high-pressure conditions.

In situ studies of the viscosity (Scarfe et al. 1987; Kushiro 1976, 1986) and diffusion rates (Rubie et al. 1993) in silicate melts have consistently documented the occurrence of major changes in transport properties from low to high pressures. However, spectroscopic studies performed on glasses quenched from high-pressure, high-temperature conditions have just as consistently revealed little or no structural differences between glasses formed at ambient pressure and those quenched from high pressure. Hence, it has been suggested that the pressure dependence of the transport properties of silicate liquids is anomalous (Sharma et al. 1979). The low-pressure (to  $\sim 5$  GPa) changes in viscosity and diffusivity are likely to be

primarily a consequence of changes in Si-O-Si angles or ring distributions. Within alkali silicates it is possible that a component of these low-pressure changes in transport properties may be produced by small amounts of coordination changes. Indeed, the linear change in the log of diffusivity between 2.5 and 10 GPa observed by Rubie et al. (1993) suggests that coordination changes may modulate anion diffusivity at pressures as low as 2.5 GPa. However, these data may be sensitive to lower abundances of highly coordinated Si. The Raman spectra presented here show a distinct signature of apparent coordination changes only above  $\sim 5$  GPa. Our results indicate that the connection of pressure-induced coordination changes to transport properties is different from what would be indicated by the structure of pressure-quenched (and tetrahedra-dominated) samples. Thus, transport properties plausibly sample a notably different liquid structure at high pressures than at low pressures, and the quenched glasses do not directly record these structural changes.

We can interpret the notable difference between the structure of the compressed glass and liquid at 8 and 10 GPa from the relative elasticity of the two phases. The bulk modulus of relaxed  $\text{Na}_2\text{Si}_2\text{O}_5$  liquid is approximately one-half that of  $\text{Na}_2\text{Si}_2\text{O}_5$  glass (20 GPa vs. 40 GPa; Kress et al. 1988; White et al. 1977). Therefore, over the pressure range of our high-pressure experiments, we expect a 5–8% increase in density of the glass upon heating (Fig. 6). The crucial point here is that the compressed glass is not the same glass that is formed from quenching the liquid at high pressures. Moreover, significant volumetric relaxation on heating (as long as it is not discontinuous) does not violate the formal second-order thermodynamic definition of the glass transition.

To correlate this density change with shifts in melt structure we construct a simple model of the density of possible crystalline assemblages of the disilicate composition as a function of Si coordination (Fig. 7). We assume that the glass contains 50% <sup>16</sup>Si at 8 GPa (the pressure at which we lose evidence of Q species) and that the density change on relaxation to the liquid state is accommodated through coordination changes only. The density change of 5–8% that should occur on relaxation of the compressed glass therefore appears to correspond to a 20–30% increase in the fraction of <sup>16</sup>Si in the liquid over that in the compressed glass at  $\sim 8$  GPa. Although the compressed glass still retains some evidence of bridged tetrahedral Si atoms at 8 GPa (implying that it may contain  $< 50\%$  <sup>16</sup>Si), we expect that the densified (and, on average, more highly coordinated) liquid at 8 GPa contains no formal Q species; this is what we observe. The complete loss of formal Q species in  $\text{Na}_2\text{Si}_2\text{O}_5$  liquid requires the formation of highly coordinated O. Thus, <sup>13</sup>O as well as <sup>16</sup>Si are formed as bridging O atoms move into the coordination sphere of formerly tetrahedral Si.

The increased intensity of the bands associated with the Q<sup>2</sup> species in a glass quenched from a high-pressure ( $P > \sim 5$  GPa) liquid relative to that quenched at ambient



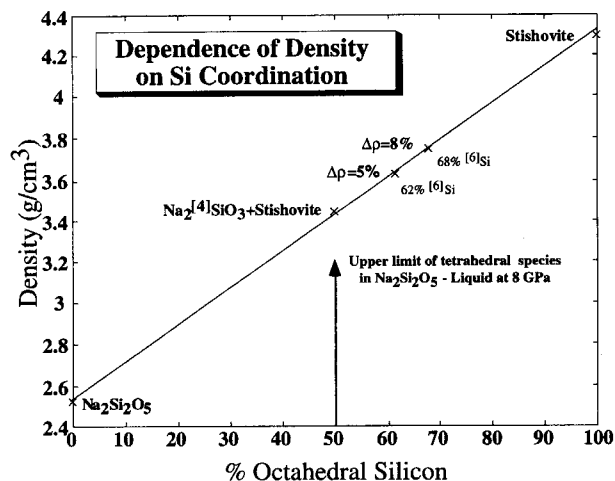


FIGURE 7. Densities of hypothetical assemblages of  $\text{Na}_2\text{Si}_2\text{O}_5$  composition as a function of octahedral Si content. The densities of the largely tetrahedral phases were estimated from a linear fit to the densities as a function of composition for seven low-pressure sodium silicate crystalline phases:  $\text{Na}_2\text{Si}_3\text{O}_7$  (Williamson and Glasser 1966);  $\text{Na}_6\text{Si}_8\text{O}_{19}$  (Williamson and Glasser 1965);  $\alpha\text{-Na}_2\text{Si}_2\text{O}_5$  (Williamson and Glasser 1966);  $\beta\text{-Na}_2\text{Si}_2\text{O}_5$  (Williamson and Glasser 1966);  $\text{Na}_2\text{SiO}_3$  (Grund and Pizy 1952);  $\text{Na}_6\text{Si}_2\text{O}_7$  (Kautz et al. 1970); and  $\text{Na}_4\text{SiO}_4$  (Olazcuaga et al. 1975). We utilize the density of stishovite as a proxy for the density of a phase containing 100%  $^{16}\text{Si}$ . This approximation should yield a lower bound on the change in  $^{16}\text{Si}$  content for a given change in density of an amorphous  $\text{Na}_2\text{Si}_2\text{O}_5$  phase. Note that we examine relative changes in density during shifts in coordination, rather than the absolute value of the density produced by different coordination environments.

pressure has been proposed to occur by means of a pressure-induced speciation change (Xue et al. 1991):  $2\text{Q}^3 \rightarrow \text{Q}^4 + \text{Q}^2$ .

However, because of both our high-temperature data and the data collected in situ on glasses under compression, we concur with Wolf et al. (1990) that such speciation changes in our glasses result only from the reversion on decompression of dense structures within the glasses. Because of the relatively low level at which this reaction occurs, we are not able to determine which structures revert to produce this speciation change; they could be highly coordinated Si or unstable dense tetrahedral configurations.

In conclusion, the Raman spectra obtained from  $\text{Na}_2\text{Si}_2\text{O}_5$  liquid at high temperatures and pressures document that major differences exist between liquids quenched to ambient conditions and their high-pressure counterparts. Specifically, in liquids examined at 8 and 10 GPa, a minimum of  $\sim 50\%$  of the Si resides in highly coordinated polyhedra ( $^{15}\text{Si}$  or  $^{16}\text{Si}$ ). Moreover, decompression-induced reversion of a structure with highly coordinated Si produces a glass at zero pressure that is only subtly different from ordinary ambient pressure glass but differs dramatically from the actual high-pressure, high-

temperature structure of the liquid. Our results suggest that the high-pressure liquid structure that gives rise to the negative pressure dependence of both anion diffusivity (Rubie et al. 1993) and density inversions between silicate liquids and coexisting solids (Stolper et al. 1981; Agee and Walker 1993) is associated with large amounts of highly coordinated Si. Because of the role that such density crossovers may have played in the development of stratification in the early Earth (Agee and Walker 1988), and in the light of new evidence for small degrees of partial melting within the deep upper mantle (Revenaugh and Sipkin 1994), we infer that coordination changes in silicate liquids plausibly play an important role in the geochemical development of both the early and modern mantle.

#### ACKNOWLEDGMENTS

We thank J. Kubicki, F. Ryerson, and two anonymous reviewers for helpful comments and Chantle Ruddle for technical assistance. This work was supported by the NSF, the IGPP at LLNL, and the W.M. Keck Foundation. We also thank M.J. Harrison for support (D.L.F.) during the preparation of this manuscript. Contribution no. 285 of the Institute of Tectonics (Mineral Physics Laboratory) at University of California, Santa Cruz.

#### REFERENCES CITED

- Agee, C.B., and Walker, D. (1988) Mass balance and phase density constraints on early differentiation of chondritic mantle. *Earth and Planetary Science Letters*, 90, 144–156.
- (1993) Olivine flotation in mantle melt. *Earth and Planetary Science Letters*, 114, 315–324.
- Angell, C.A., and Sichina, W. (1976) Thermodynamics of the glass transition: Empirical aspects. *Annals of the New York Academy of Sciences*, 279, 53–67.
- Angell, C.A., Cheeseman, P.A., and Tamaddon, S. (1982) Water-like transport property anomalies in liquid silicates investigated at high  $T$  and  $P$  by computer simulation techniques. *Bulletin de Minéralogie*, 106, 87–97.
- Barrio, R.A., Galeener, F.L., Martínez, E., and Elliott, R.J. (1993) Regular ring dynamics in  $\text{AX}_2$  tetrahedral glasses. *Physical Review B*, 48, 15672–15687.
- Brandriss, M.E., and Stebbins, J.F. (1988) Effects of temperature on the structures of silicate liquids:  $^{29}\text{Si}$  NMR results. *Geochimica et Cosmochimica Acta*, 52, 2659–2669.
- Brawer, S.A. (1985) Relaxation in viscous liquids and glasses, 220 p. American Ceramic Society, Columbus, Ohio.
- Brawer, S.A., and White, W.B. (1975) Raman spectroscopic investigation of the structure of silicate glasses: I. The binary silicate glasses. *Journal of Chemical Physics*, 63, 2421–2432.
- Burnham, C.W. (1981) The nature of multicomponent aluminosilicate melts. In D.T. Rickard and F.E. Wickman, Eds., *Chemistry and geochemistry of solutions at high temperatures and pressures*, p. 197–229. Pergamon, New York.
- Closmann, C., and Williams, Q. (1995) In-situ spectroscopic investigation of high-pressure hydrated (Mg,Fe)SiO<sub>3</sub> glasses: OH vibrations as a probe of glass structure. *American Mineralogist*, 80, 201–212.
- Dickinson, J., Jr., Scarfe, C.M., and McMillan, P.F. (1990) Physical properties and structure of  $\text{K}_2\text{Si}_2\text{O}_7$  melt quenched from pressures up to 2.4 GPa. *Journal of Geophysical Research*, 95, 15675–15681.
- Durban, D.J., and Wolf, G.H. (1991) Raman spectroscopic study of the pressure-induced coordination change in  $\text{GeO}_2$  glass. *Physical Review B*, 43, 2355–2363.
- Farber, D.L., and Williams, Q. (1992) Pressure-induced coordination changes in alkali-germanate melts: An in situ spectroscopic investigation. *Science*, 256, 1427–1430.
- Furukawa, T., Fox, K.E., and White, W.B. (1981) Raman spectroscopic investigation of the structure of silicate glasses: III. Raman intensities

- and the structural units in sodium silicate glasses. *Journal of Chemical Physics*, 75, 3226–3237.
- Galeener, F.L. (1982) Planar rings in vitreous silica. *Journal of Non-Crystalline Solids*, 49, 53–62.
- Galeener, F.L., and Mikkelsen, J.C. (1981) Vibrational dynamics in  $^{18}\text{O}$ -substituted vitreous  $\text{SiO}_2$ . *Physical Review B*, 23, 5527–5530.
- Galeener, F.L., and Geissberger, A.E. (1983) Vibrational dynamics in  $^{30}\text{Si}$ -substituted vitreous  $\text{SiO}_2$ . *Physical Review B*, 27, 6199–6204.
- Grund, P.A., and Pizy, M.M. (1952) Structure cristalline du metasilicate de sodium anhydre,  $\text{Na}_2\text{SiO}_3$ . *Acta Crystallographica*, 5, 837–840.
- Gupta, P.K. (1987) Negative pressure dependence of viscosity. *Journal of the American Ceramic Society*, 70, c152–c153.
- Hemley, R.J. (1987) Pressure dependence of Raman spectra of  $\text{SiO}_2$  polymorphs:  $\alpha$ -quartz, coesite, and stishovite. In M. Manghni and Y. Sono, Eds., *High pressure research in mineral physics*, p. 347–361. American Geophysical Union, Washington, DC.
- Hemley, R.J., Mao, H.K., and Chao, E.C. (1986a) Raman spectrum of natural and synthetic stishovite. *Physics and Chemistry of Minerals*, 13, 285–290.
- Hemley, R.J., Mao, H.K., Bell, P.M., and Mysen, B.O. (1986b) Raman spectroscopy of  $\text{SiO}_2$  glass at high pressures. *Physical Review Letters*, 747–750.
- Hess, N.J., and Schiferl, D.S. (1990) Pressure and temperature dependence of laser induced fluorescence of Sm:YAG to 100 kb and 700 °C and an empirical model. *Journal of Applied Physics*, 68, 1953–1960.
- Irfune, I., and Ohtani, E. (1986) Melting of pyrope  $\text{Mg}_3\text{Al}_2\text{Si}_3\text{O}_{12}$  up to 10 GPa: Possibility of a pressure-induced structural change in pyrope melt. *Journal of Geophysical Research*, 91, 9357–9366.
- Itie, J.P., Polian, A., Calas, G., Petiau, J., Fontaine, A., and Tolentino, H. (1989) Pressure-induced coordination changes in crystalline and vitreous  $\text{GeO}_2$ . *Physical Review Letters*, 63, 398–401.
- Kanzaki, M., Xue, X., and Stebbins, J. (1989) High pressure phase relations in  $\text{Na}_2\text{Si}_2\text{O}_7$ ,  $\text{Na}_2\text{Si}_2\text{O}_6$ , and  $\text{K}_2\text{Si}_4\text{O}_9$  up to 12 GPa. *Eos*, 70, 1418.
- Kautz, K., Müller, G., and Schneider, W. (1970) Determination of the lattice constants and space groups of sodium orthosilicate ( $\text{Na}_4\text{SiO}_4$ ) and sodium pyrosilicate ( $\text{Na}_2\text{Si}_2\text{O}_7$ ) and investigation of their range of stability by a high temperature camera. *Glastechnische Berichte*, 43, 377–381.
- Knittle, E., and Jeanloz, R. (1989) Melting curve of  $(\text{Mg},\text{Fe})\text{SiO}_3$  perovskite to 96 GPa: Evidence for a structural transition in the lower mantle. *Geophysical Research Letters*, 16, 421–424.
- Kraft, S., Knittle, E., and Williams, Q. (1991) Carbonate stability in the Earth's mantle: A vibrational spectroscopic study of aragonite and dolomite at high pressures and temperatures. *Journal of Geophysical Research*, 96, 17997–18009.
- Kress, V.C., Williams, Q., and Carmichael, I.S.E. (1988) Ultrasonic investigation of melts in the system  $\text{Na}_2\text{O}-\text{Al}_2\text{O}_3-\text{SiO}_2$ . *Geochimica et Cosmochimica Acta*, 52, 283–293.
- (1989) When is a silicate melt not a liquid? *Geochimica et Cosmochimica Acta*, 53, 1687–1692.
- Kubicki, J.D., and Lasaga, A.C. (1991) Molecular dynamics simulations of pressure and temperature effects on  $\text{MgSiO}_3$  and  $\text{Mg}_2\text{SiO}_4$  melts and glasses. *Physics and Chemistry of Minerals*, 17, 661–673.
- Kubicki, J.D., and Sykes, D. (1993) Molecular orbital calculations of the vibrations in 3-membered aluminosilicate rings. *Physics and Chemistry of Minerals*, 19, 381–391.
- Kushiro, I. (1976) Changes in viscosity and structure of melt of  $\text{NaAlSi}_3\text{O}_8$  composition at high pressures. *Journal of Geophysical Research*, 81, 6347–6350.
- (1980) Viscosity, density, and structure of silicate melts at high pressures, and their petrological applications. In R.B. Hargraves, Ed., *Physics of magmatic processes*, p. 93–120. Princeton University Press, Princeton, New Jersey.
- (1986) Viscosity of partial melts in the upper mantle. *Journal of Geophysical Research*, 91, 9343–9350.
- Matson, D.W., Sharma, S.K., and Philpotts, J.A. (1983) The structure of high-silica alkali-silicate glasses: A Raman spectroscopic investigation. *Journal of Non-Crystalline Solids*, 58, 323–352.
- Matsui, Y., Kawamura, K., and Syono, Y. (1982) Molecular dynamics calculations applied to silicate systems: Molten and vitreous  $\text{MgSiO}_3$  and  $\text{Mg}_2\text{SiO}_4$  under low and high pressures. In S. Akimoto and M. Manghni, Eds., *High pressure research in geophysics*, p. 511–524. Center for Academic Publishing, Tokyo.
- McMillan P. (1984) Structural studies of silicate glasses and melts: Applications and limitations of Raman spectroscopy. *American Mineralogist*, 69, 622–644.
- McMillan, P.F., and Ross, N. (1987) Heat capacity calculations for  $\text{Al}_2\text{O}_3$  corundum and  $\text{MgSiO}_3$  ilmenite. *Physics and Chemistry of Minerals*, 14, 225–234.
- McMillan, P.F., Poe, B.T., Gillet, P., and Reynard, B. (1994) A study of  $\text{SiO}_2$  glass and supercooled liquid to 1950 K via high-temperature Raman spectroscopy. *Geochimica et Cosmochimica Acta*, 58, 3653–3664.
- Meade, C., Hemley, R.J., and Mao, H.K. (1992) High-pressure X-ray diffraction of  $\text{SiO}_2$  glass. *Physical Review Letters*, 69, 1387–1390.
- Miller, G.H., Stolper, E.M., and Ahrens, T.J. (1991) The equation of state of a molten komatiite: 2. Application to komatiite petrogenesis and the Hadean mantle. *Journal of Geophysical Research*, 96, 11849–11864.
- Mills, J.J. (1972) Low frequency storage and loss moduli of soda-silica glasses in the transformation range. *Journal of Non-Crystalline Solids*, 14, 255–268.
- Mysen, B.O. (1990) Relationships between melt structure and petrologic processes. *Earth-Science Reviews*, 27, 261–365.
- Mysen, B.O., and Frantz, J.D. (1993) Structure and properties of alkali silicate melts at magmatic temperatures. *European Journal of Mineralogy*, 5, 393–407.
- (1994) Alkali silicate glass and melt structure in the temperature range 25–1651 °C at atmospheric pressure and implications for mixing behavior of structural units. *Contributions to Mineralogy and Petrology*, 117, 1–14.
- Olazcuaga, R., Reau, J., Devalette, M., Le Flem, G., and Hagenmuller, P. (1975) Les phases  $\text{Na}_4\text{XO}_4$  (X = Si, Ti, Cr, Mn, Co, Ge, Sn, Pb) et  $\text{K}_4\text{XO}_4$  (X = Si, Ti, Cr, Mn, Co, Ge, Sn, Pb). *Journal of Solid State Chemistry*, 13, 275–282.
- Revenaugh, J., and Sipkin, S.A. (1994) Seismic evidence of silicate melt atop the 410-km mantle discontinuity. *Nature*, 369, 474–476.
- Revesz, A.G., and Walrafen, G.E. (1983) Structural interpretations for some lines from vitreous silica. *Journal of Non-Crystalline Solids*, 54, 323–333.
- Rigden, S.M., Ahrens, T.J., and Stolper, E.M. (1984) Densities of liquid silicates at high pressures. *Science*, 226, 1071–1074.
- (1988) Shock compression of a molten silicate: Results for a model basaltic composition. *Journal of Geophysical Research*, 93, 367–382.
- Rosenhauer, M., Scarfe, C.M., and Virgo, D. (1978) Pressure dependence of the glass transition temperature in glasses of diopside, albite, and sodium trisilicate composition. *Carnegie Institution of Washington Year Book*, 78, 556–559.
- Rubie, D.C., Ross, C.R., II, Carroll, M.R., and Elphick, S.C. (1993) Oxygen self-diffusion on  $\text{Na}_4\text{Si}_4\text{O}_9$  liquid up to 10 GPa and estimation of high-pressure melt viscosities. *American Mineralogist*, 78, 574–582.
- Rustad, J.R., Yuen, D.A., and Spera, F.J. (1990) Molecular dynamics of liquid  $\text{SiO}_2$  under high pressure. *Physical Review A*, 42, 2081–2089.
- (1991) The statistical geometry of amorphous silica at lower-mantle pressures: Implications for melting slopes of silicates and anharmonicity. *Journal of Geophysical Research*, 96, 19665–19672.
- Ryerson, F.J., and Hess, P.C. (1978) Implications of liquid-liquid distribution coefficients to mineral-liquid partitioning. *Geochimica et Cosmochimica Acta*, 42, 921–932.
- Scarfe, C.M., Mysen, B.O., and Virgo, D. (1978) Changes in viscosity and density of melts of sodium disilicate, sodium metasilicate, and diopside composition with pressure. *Carnegie Institution of Washington Year Book*, 78, 547–551.
- (1987) Pressure dependence of the viscosity of silicate melts. In B.O. Mysen, Ed., *Magmatic processes: Physicochemical principles*, p. 59–68. Geochemical Society, Special Publication no. 1.
- Sharma, S.K., Virgo, D., and Kushiro, I. (1979) Relationship between density, viscosity and structure of  $\text{GeO}_2$  melts at low and high pressures. *Journal of Non-Crystalline Solids*, 33, 235–248.
- Sharma, S.K., Mammone, J.F., and Nicol, M.F. (1981) Raman investigation of ring configurations in vitreous silica. *Nature*, 292, 140–141.
- Shimizu, N., and Kushiro, I. (1984) Diffusivity of oxygen in jadeite and

- diopside melts at high pressures. *Geochimica et Cosmochimica Acta*, 48, 1295–1303.
- Stebbins, J.F., and Farnan, I. (1989) Nuclear magnetic resonance spectroscopy in the earth sciences: Structure and dynamics. *Science*, 245, 257–263.
- Stolper, E.M., Walker, D., Hager, B.H., and Hays, J.F. (1981) Melt segregation from partially molten source regions: The importance of melt density and source region size. *Journal of Geophysical Research*, 86, 6261–6271.
- Sweet, J.R., and White, W.B. (1969) Study of sodium silicate glasses and liquids by infrared reflectance spectroscopy. *Physics and Chemistry of Glasses*, 10, 246–251.
- Tischer, R.E., and Drickamer, H.G. (1962) Use of pressure to investigate symmetry and compressibility in glass. *Journal of Chemical Physics*, 37, 1554–1562.
- Uhlmann, D.R. (1973/1974) Densification of alkali silicate glasses at high pressure. *Journal of Non-Crystalline Solids*, 13, 89–99.
- Watson, E.B. (1977) Partitioning of manganese between forsterite and silicate liquid. *Geochimica et Cosmochimica Acta*, 41, 1363–1374.
- (1979) Calcium diffusion in a simple silicate melt to 30 kbar. *Geochimica et Cosmochimica Acta*, 43, 205–256.
- White, G.K., Birch, J.A., and Manghnani, M.H. (1977) Thermal properties of sodium silicate glasses at low temperatures. *Journal of Non-Crystalline Solids*, 23, 99–110.
- Williams, Q., Jeanloz, R., and McMillan, P. (1987) Vibrational spectrum of MgSiO<sub>3</sub> perovskite: Zero-pressure Raman and mid-infrared spectra to 27 GPa. *Journal of Geophysical Research*, 92, 8116–8128.
- Williams, Q., and Jeanloz, R. (1988) Spectroscopic evidence for pressure induced coordination changes in silicate glasses and melts. *Science*, 239, 902–905.
- (1989) Static amorphization of anorthite at 300 K and comparison with diaplectic glass. *Nature*, 338, 413–415.
- Williams, Q., Hemley, R.J., Kruger, M.B., and Jeanloz, R. (1993) High-pressure infrared spectra of  $\alpha$ -quartz, coesite, stishovite, and silica glass. *Journal of Geophysical Research*, 98, 22157–22170.
- Williamson, J., and Glasser, F.P. (1965) Phase relations in the system Na<sub>2</sub>Si<sub>2</sub>O<sub>5</sub>-SiO<sub>2</sub>. *Science*, 148, 1589–1591.
- (1966) The crystallisation of Na<sub>2</sub>O·2SiO<sub>2</sub>-SiO<sub>2</sub> glasses. *Physics and Chemistry of Glasses*, 7, 127–138.
- Wolf, G.H., Durban, D.J., and McMillan, P.F. (1990) High-pressure Raman spectroscopic study of sodium tetrasilicate (Na<sub>2</sub>Si<sub>4</sub>O<sub>8</sub>) glass. *Journal of Chemical Physics*, 93, 2280–2288.
- Xue, X., Stebbins, J.F., Kanzaki, M., McMillan, P.F., and Poe, B. (1991) Pressure-induced silicon coordination and tetrahedral structural changes in alkali oxide-silica melts up to 12 GPa: NMR, Raman, and infrared spectroscopy. *American Mineralogist*, 76, 8–26.
- Xue, X., Stebbins, J.F., and Kanzaki, M. (1993) A <sup>29</sup>Si MAS NMR study of sub-*T<sub>g</sub>* amorphization of stishovite at ambient pressure. *Physics and Chemistry of Minerals*, 19, 480–485.
- Zanotto, E.D., and Weinberg, M.C. (1989) Trends in homogeneous crystal nucleation in oxide glasses. *Physics and Chemistry of Glasses*, 30, 186–192.

MANUSCRIPT RECEIVED OCTOBER 27, 1994

MANUSCRIPT ACCEPTED NOVEMBER 21, 1995